ARTICLES

Photophysical Properties and Singlet Oxygen Production by Ruthenium(II) Complexes of Benzo[*i*]dipyrido[3,2-*a*:2′,3′-*c*]phenazine: Spectroscopic and TD-DFT Study

Simon P. Foxon, Mohammed A. H. Alamiry, Mike G. Walker, Anthony J. H. M. Meijer,* Igor V. Sazanovich, Julia A. Weinstein,* and James A. Thomas*

Department of Chemistry, University of Sheffield, Sheffield S3 7HF, United Kingdom

Received: July 16, 2009; Revised Manuscript Received: September 10, 2009

The photophysical properties of a series of Ru^{II} complexes containing benzo[*i*]dipyrido[3,2-*a*:2′,3′-*c*]phenazine (dppn) as a ligand are reported. Transient absorption spectroscopy studies indicate that, in contrast to related Ru(dppz) complexes (dppz = dipyrido[3,2-*a*:2′,3′-*c*]phenazine), the excited state of all the dppn systems is a long-lived $\pi\pi^*$ triplet state. Computational studies (DFT and TD-DFT) confirm that the excited state is based on the dppn ligand. Near-infrared luminescence studies reveal that the complexes are efficient singlet oxygen sensitizers with yields of 70−83%.

Introduction

Over the past two decades, the number of studies on metal complexes that reversibly bind to nucleic acids has rapidly grown. These systems bind through a combination of interactions commonly observed for classical DNA binding substrates, such as electrostatics, groove binding, and intercalation between base pairs.[1,2] Complexes that bind with sequence[3] and structural[4] selectivity have been reported, and up to nanomolar binding affinities[5] have been achieved. Due to their rich redox and photochemical properties, the incorporation of transition-metal centers within these architectures can also enhance their functionality. Perhaps the best known class of metal-complex-based DNA intercalators are those based on [M(dppz)] moieties (where M = a d^6 metal ion), with the prototypes being the much studied DNA lights switches $[Ru(bpy)_2(dppz)]^{2+}$ and $[Ru(phen)_2(dppz)]^{2+}$ (where bpy = 2,2′-bipyridine and phen = 1,10-phenanthroline).[6] These complexes only display the characteristic ^{3}MLCT emission of polypyridyl-Ru^{II} systems in nonprotic solvents. In aqueous solutions, excited-state emission is quenched; however, on DNA intercalation, dppz inserts into the more hydrophobic environment of the base pair stack, causing $Ru^{II} \rightarrow$ dppz-based ^{3}MLCT emission to reoccur.[7] This phenomenon is modulated when dppz is coordinated to other metal ions. For example, while $[Os(bpy)_2(dppz)]^{2+}$ displays red shifting in its light-switch effect compared to the Ru^{II} complexes,[8] research has revealed that the Re^{I} complex $[Re(CO)_3(py)(dppz)]^+$ (where py = pyridine or picoline), $\mathbf{1}^+$, has very different excited-state properties.[9] Initial studies by the Schanze[9] and Yam[10] groups showed that this complex also displayed a light-switch effect, and although the emission enhancements were greatly diminished compared to those of the Ru^{II}-based systems, the Re^{I} complex was capable of cleaving DNA. These studies also suggested that photoexcitation of $\mathbf{1}^+$ resulted in population and equilibration between the expected Re → dppz-based ^{3}MLCT and a longer lived dppz-centered $\pi \rightarrow \pi^*$ excited state. Consequently, detailed time-resolved IR studies indicated that an initially populated dppz-based $^1\pi \rightarrow \pi^*$ state and a ^{1}MLCT state localized on the phen fragment of dppz relax into a $^3\pi \rightarrow \pi^*$ state centered on the phenazine section of dppz, which is in equilibrium with a close-lying Re → dppz ^{3}MLCT also located on the phenazine fragment.[11,12] When the mechanism of DNA cleavage was investigated, it was concluded that, whereas the related complex $[Re(CO)_3(py)(dppn)]^+$, $\mathbf{2}^+$ (where dppn = benzo[*i*]dipyrido[3,2-*a*:29,39-*c*]phenazine), which did not show a light-switch effect, indirectly cleaves DNA through singlet oxygen sensitization, complex $\mathbf{1}^+$ directly cleaves DNA at guanine sites.[13] In fact, despite the huge amount of research into dppz-based systems, this latter study is one of the few to investigate the properties of complexes containing dppn. This is probably because, in the 1992 report that first described the synthesis of the ligand, Hartshorn and Barton revealed that $[Ru(phen)_2(dppn)]^{2+}$ does not display a light-switch effect on binding with DNA.[14]

In previous work, to facilitate the future construction of higher order structures with defined chirality, we have described a modular synthesis of oligomeric metallointercalators, in which achiral building blocks such as the $[Ru(tpm)(dppz)(L)]^{2+}$ unit (tpm = tris-(1-pyrazolyl)methane, L = N-donor ligands) were used to construct homo- and heterodinuclear systems.[15−17] In this work we also noted that $[Ru(tpm)(dppn)(L)]^{2+}$ complexes showed poor emission properties and no light-switch effect. These observations—and those by the Yam group on $\mathbf{1}^+$ and $\mathbf{2}^+$—suggest that the photoexcited states of M(dppn) complexes are generally different from those of M(dppz) systems. This prompted us to further investigate the differences between the excited states of the analogous $[Ru^{II}(dppz)]$ and $[Ru^{II}(dppn)]$ units, in the hope that their properties could be exploited in the assembly of multifunctional oligonuclear systems.

Results and Discussion

The complexes $\mathbf{1}^+$, $\mathbf{2}^+$, and $[Ru(bpy)_2(dppn)]^{2+}$, $\mathbf{3}^{2+}$, and the previously reported $[Ru(tpm)(MeCN)(dppn)]^{2+}$, $\mathbf{4}^{2+}$, and [Ru(tp-

* To whom correspondence should be addressed. E-mail: A.Meijer@sheffield.ac.uk (A.J.H.M.M.); james.thomas@sheffield.ac.uk (J.A.T.); Julia.Weinstein@sheffield.ac.uk (J.A.W.).

10.1021/jp906716g CCC: $40.75
Published on Web 09/30/2009

SCHEME 1: Complexes Relevant to This Study

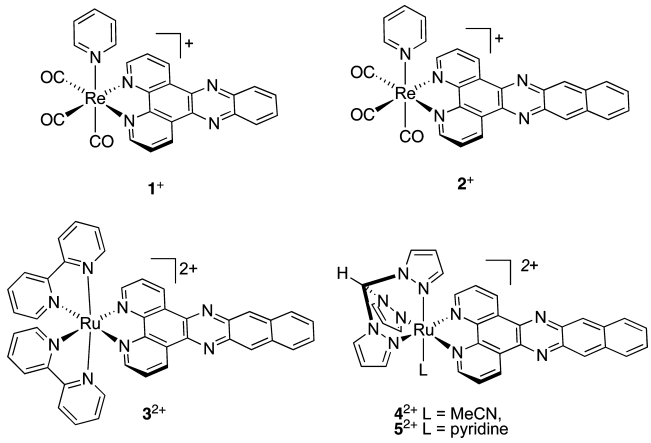

m)(py)(dppn)]$^{2+}$, $\mathbf{5}^{2+}$ (where py = pyridine), Scheme 1, were synthesized using literature methods.[9,10,14−16,19]

The ground-state electronic absorption spectra for complexes $\mathbf{4}^{2+}$ and $\mathbf{5}^{2+}$ have been reported previously. The spectra of $\mathbf{3}^{2+}$ in CH_3CN (as a PF_6^- salt) and in water (as a chloride salt) are shown in Figure 1, and relevant data are summarized in Table 1.

As for $\mathbf{4}^{2+}$ and $\mathbf{5}^{2+}$, the absorption spectrum of $\mathbf{3}^{2+}$ shows intense intraligand (π, π^*) absorption bands in the UV region ($\lambda < 350$ nm) with less intense absorption bands in the visible range, ca. 350−550 nm. While the lowest Ru → dppn-based ^{1}MLCT absorption band occurs at 477 nm for $\mathbf{4}^{2+}$ and 449 nm for $\mathbf{5}^{2+}$ in CH_3CN, for $\mathbf{3}^{2+}$ the lowest energy absorption manifold is clearly an overlap of several transitions. (Figure 1, Table 1), from which transitions at 387, 409, 443, 492, and 525 nm can be extracted by Gaussian deconvolution. The different spectral profile of $\mathbf{3}^{2+}$ compared to $\mathbf{4}^{2+}$ and $\mathbf{5}^{2+}$ can be attributed to an overlap of Ru−dppn ^{1}MLCT and Ru−bpy ^{1}MLCT manifolds. The detailed assignment of the manifold of frontier orbitals is given in the "DFT Calculations" section of this paper. In agreement with previous studies on dppn-based systems, $\mathbf{3}^{2+}$,

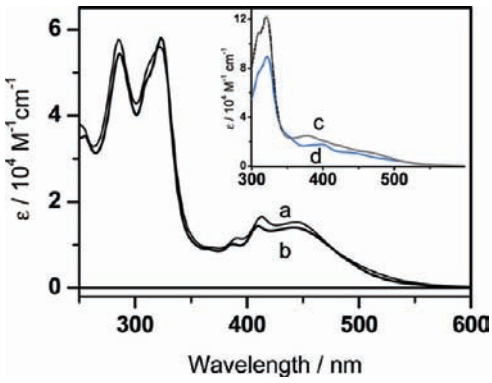

Figure 1. Ground-state electronic absorption spectra of $\mathbf{3}^{2+}$ in water (a, thin solid line) and CH_3CN (b, thick solid line). Inset: ground-state electronic absorption spectra of $\mathbf{5}^{2+}$ (c) and $\mathbf{4}^{2+}$ (d) in CH_3CN.

TABLE 1: Absorption Spectra of $\mathbf{3}^{2+}$ at Room Temperature in MeCN and Water

solvent	λ/nm ($10^{-3}\varepsilon$/M^{-1} cm^{-1})
MeCN[a]	286 (54.4), 323 (58.1), 338 (22.4), 387 (10.2), 409 (14.3), 443 (14.0)
water[b]	285 (57.1), 322 (55.2), 412 (16.6), 443 (11.9)

[a] Hexafluorophosphate. [b] Chloride salt.

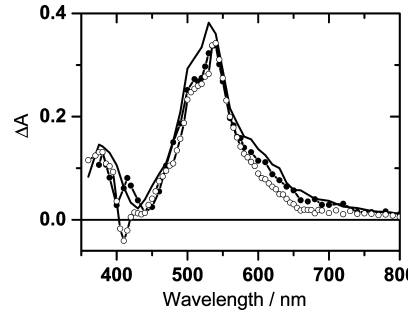

Figure 2. Zero-time transient absorption spectra of $\mathbf{3}^{2+}$ (○), $\mathbf{4}^{2+}$ (solid line), and $\mathbf{5}^{2+}$ (●) in MeCN under 355 nm excitation.

$\mathbf{4}^{2+}$, and $\mathbf{5}^{2+}$ do not display the characteristically intense ^{3}MLCT-based luminescence observed for $[Ru(LL)_2(dppz)]^{2+}$ complexes; this observation raises questions about the exact nature of the lowest excited state in dppn complexes of Ru^{II} compared to that of dppz-based light-switch systems.

It is postulated that the light-switch effect of $[Ru(LL)_2(dppz)]^{2+}$ systems is due to interplay between excited states.[20−25] While the emissive "bright state" has been assigned as a ^{3}MLCT, the nature of the "dark state" is debated. Initially it was hypothesized that the dark state was a second ^{3}MLCT centered on the phenazine unit of dppz; however, later theoretical studies have pointed to the involvement of a $\pi \rightarrow \pi^*$ excited state also located on the phenazine moiety.[26] The photophysical properties of $\mathbf{3}^{2+}$−$\mathbf{5}^{2+}$ hint that for Ru^{II}(dppn) systems an excited state related to the Ru^{II}(dppz) dark state is always the favored excited state. To investigate this issue, the nature of the lowest excited state was probed through transient absorption studies and the spectra obtained were compared with the results of the DFT calculations, vide infra.

Nanosecond Transient Absorption Studies. Studies were performed in the range 370−800 nm. The transient difference spectra obtained in flash photolysis experiments for complexes $\mathbf{3}^{2+}$−$\mathbf{5}^{2+}$ in MeCN are shown in Figure 2.

Excitation of solutions of all three complexes with a 7 ns laser pulse at 355 nm leads to bleaching of the absorption bands of the ground state and to the formation of several transient bands. The transient spectra for $\mathbf{3}^{2+}$−$\mathbf{5}^{2+}$ are virtually identical; in particular, intense transient absorptions in the 450−700 nm region with a pronounced maximum at ca. 540 nm and a smaller maximum at ca. 375 nm are observed. These data imply that the lowest excited state detected on the nanosecond time scale is the same in all cases. The dips in the transient spectra at ca. 410−440 nm correspond to bleaching of the ground-state MLCT band.

The generated transient bands decay in a monoexponential fashion, Figure 3, Table 2. The lifetimes of the lowest excited state of all three complexes in deoxygenated acetonitrile are in the tens of microseconds range, which is clearly considerably longer than the 180 ns lifetime of the emissive excited state of $[Ru(bpy)_2(dppz)]^{2+}$ in the same solvent.[7] We conclude that the transient data suggest that, for all three Ru^{II}(dppn) complexes, the common nonemissive excited state is triplet in nature, although—given its long lifetime—it seems unlikely that this state is closely analogous to the dark state observed for Ru(dppz) systems. We then proceeded to investigate the effect of the solvent on the excited state.

Time-resolved spectroscopy in water has revealed that the $[Ru(bpy)_2(dppz)]^{2+}$ light switch is "off" in protic solvents due to rapid conversion ($\tau \approx 3$ ps) of the light state into the dark excited state, which then rapidly deactivates by a radiationless

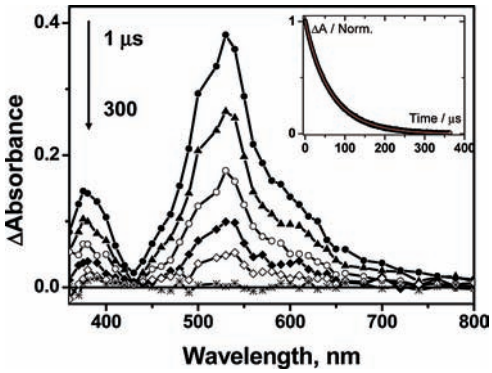

Figure 3. Typical transient absorption spectra for $\mathbf{4}^{2+}$ at different time delays after the laser excitation with a 355 nm, 7 ns pulse. The inset shows a kinetic trace at 530 nm and a monoexponential fit to this data (red line).

TABLE 2: Excited-State Lifetimes of Complexes $\mathbf{3}^{2+}$−$\mathbf{5}^{2+}$ Obtained by Flash Photolysis

	lifetime (μs)	
complex	MeCN	water
$\mathbf{3}^{2+}$	62 ± 5	11.9 ± 1.0
$\mathbf{4}^{2+}$	74 ± 5	25 ± 3
$\mathbf{5}^{2+}$	35 ± 3	0.23 ± 0.02

pathway. It was originally suggested that the dark state became energetically favored through stabilization by H-bonding with water molecules.[20−23] However, variable-temperature studies reported by Brennaman et al. suggest an equilibrium between the light and dark states even in *aprotic* solvents.[24,25] As a consequence, the researchers hypothesized that the dark state is always lower in energy and the light state is accessed through entropic factors.[26] Given the subtleties of these effects, we investigated whether the long-lived excited state of [Ru(dppn)] was affected by water solvation.

The PF_6^- salts of $\mathbf{3}^{2+}$, $\mathbf{4}^{2+}$, and $\mathbf{5}^{2+}$ were converted into water-soluble chlorides by anion metathesis with tetrabutylammonium chloride, and transients for the complexes were recorded in aqueous solution. As Figure 4—showing the consequences of photoexciting $\mathbf{4}^{2+}$—illustrates, the shapes of the transient spectra in water are virtually identical to those in MeCN.

However, the lifetime of the excited state is affected by the solvent and shows a marked decrease in the case of $\mathbf{3}^{2+}$ and $\mathbf{4}^{2+}$ and a dramatic decrease by 2 orders of magnitude in the case of $\mathbf{5}^{2+}$ in water vs CH_3CN. The effect of water on the excited-state lifetimes is illustrated in Figure 5 for the example of $\mathbf{4}^{2+}$. The Schanze group have observed that the dppz-based $^3\pi\pi^*$ state of $\mathbf{1}^+$ is short-lived in water, due to deactivation through internal conversion to a second close-lying triplet state which decays through a nonradiative mechanism.[9] The present

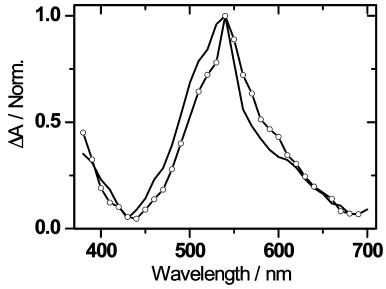

Figure 4. Zero-time normalized transient absorption spectra of $\mathbf{4}^{2+}$ in MeCN (solid line) and water (o) under 355 nm excitation.

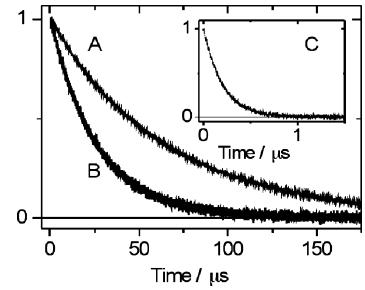

Figure 5. Normalized transient absorption decay kinetics for deoxygenated solutions of $\mathbf{4}^{2+}$ in MeCN (A), in water (B), and in air-equilibrated MeCN (C) obtained in the maximum of the transient spectrum at 540 nm under 355 nm excitation.

SCHEME 2: Structure of pydppn

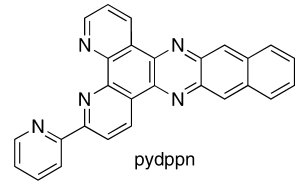

studies suggest a somewhat similar process may be involved with these Ru^{II}(dppn) systems.

Interestingly, while we were carrying out these spectral studies on $\mathbf{3}^{2+}$, $\mathbf{4}^{2+}$, and $\mathbf{5}^{2+}$, the Turro and Thummel groups reported very similar spectra for the complexes $[Ru(pydppn)_2]^{2+}$ and $[Ru(tpy)(pydppn)]^{2+}$, where tpy is 2,2′:6′,2″-terpyridine and pydppn is a tridentate analogue of the dppn ligand—3-(pyrid-2′-yl)-4,5,9,16-tetraazadibenzo[*a*,*c*]naphthacene, Scheme 2.[27] Through detailed spectroscopic studies, these spectra were assigned to a $^3\pi-\pi^*$ intraligand state of the coordinated pydppn ligand, formed via a ^{3}MLCT state which itself originates from an initially populated $^1\pi\pi^*$ or ^{1}MLCT (Ru−pydppn) state.[27]

The results from our transient absorption studies and the close structural analogy with the pydppn-based systems suggest that the lowest excited state in $\mathbf{3}^{2+}$, $\mathbf{4}^{2+}$, and $\mathbf{5}^{2+}$ can also be assigned to the intra-dppn $^3\pi\pi^*$ excited state. The efficient formation of a triplet excited state in these complexes could be anticipated due to heavy atom effects. This assignment is also consistent with the long lifetime detected for those species in deoxygenated solutions.

It should be emphasized that the excited-state decay of the dppn complexes becomes faster and multiexponential with an increase in either complex concentration or laser excitation power. For example, the lifetime of the excited state of $\mathbf{5}^{2+}$ in CH_3CN decreases from 35 to 25 μs when the concentration of the sample is increased from 4.76 to 24 μM. This observation is due to self-quenching effects, commonly observed for complexes with extended flat aromatic ligands. Therefore, lifetimes given in Table 2 are reported at the lowest possible concentrations and laser powers, as described in detail in the Experimental Section.

To further confirm the triplet nature of the lowest excited state, flash photolysis was performed in air-equilibrated CH_3CN. A representative example with $\mathbf{4}^{2+}$ is shown in Figure 5C. Although transient spectra identical in shape to that obtained for the deoxygenated sample are observed, in the presence of air, the excited-state lifetime of $\mathbf{4}^{2+}$ decreases by almost 2.5 orders of magnitude, from 74 to 0.20 μs, Figure 5C. Since the concentration of dioxygen in acetonitrile is 2.42 mmol,[28] using the Stern−Volmer equation, the quenching rate constant can be estimated as approximately 2×10^9 M^{-1} s^{-1}.

TABLE 3: Yields of $^1O_2$ Generation in Aerated Acetonitrile under 355 nm Excitation

complex	yield[a] of $^1O_2$, %
$\mathbf{3}^{2+}$	83
$\mathbf{4}^{2+}$	75
$\mathbf{5}^{2+}$	70
$[Ru(tpm)(CH_3CN)(dppz)]^{2+}$	2.3

[a] In CH_3CN, aerated solutions. The yields are measured relative to a solution of a standard compound—phenalenone—of matching absorbance (0.2 in 1 cm).

Again, these observations are consistent with an excited state of triplet nature and suggest that the dppn-based metal complexes could be efficient singlet oxygen sensitizers. To investigate this hypothesis, time-resolved NIR luminescence studies were carried out.

Singlet Oxygen Sensitization. The efficiency of the $[Ru^{II}(dppn)]$ complexes toward singlet oxygen sensitization was assessed by the direct measurement of $^1O_2$ near-infrared luminescence. Irradiation of aerated solutions of complexes was accompanied by the generation of singlet oxygen, as indicated by the appearance of a characteristic $O_2(^1\Delta_g) \rightarrow {}^3O_2$ phosphorescence at 1270 nm. The yield of the formation of $^1O_2$, $\phi(^1O_2)$, was determined by measuring its phosphorescence intensity using an optically matched solution of phenalenone as a reference sensitizer.

Using the same conditions, $[Ru(tpm)(CH_3CN)(dppz)]^{2+}$, $\mathbf{6}^{2+}$, was also investigated, and the results are summarized in Table 3. In agreement with previous studies[29] on $[Ru(bpy)_2(dppz)]^{2+}$, it was found that photoexcitation of $\mathbf{6}^{2+}$ led to very little $^1O_2$ generation, confirming that Ru(dppz) systems are poor singlet oxygen sensitizers. In contrast, photoexcitation of all the complexes containing coordinated dppn ligand produced O_2 with high yields. Furthermore, the phosphorescence lifetimes of singlet oxygen produced by the complexes and by the reference sensitizer phenalenone were the same ($\sim$80 μs), confirming that $^1O_2$ does not react with the ground state of the Ru(dppn) complexes.

The high yields of $^1O_2$ are consistent with the long lifetime of the lowest excited state and its triplet nature. These results suggest a reason for the recent finding that $\mathbf{3}^{2+}$ is appreciably more cytotoxic toward HT-29 and MC-7 cell lines when compared to several other complexes[30] including $[Ru(bpy)_3]^{2+}$ and $[Ru(bpy)_2(dppz)]^{2+}$.

DFT Calculations. To further investigate the nature of the photoexcited state of the Ru^{II}(dppn)-based complexes in CH_3CN, calculations were performed as described in the Experimental Section. Minimum energy structures for $\mathbf{3}^{2+}$—$\mathbf{5}^{2+}$ were calculated, and the details are given in *xyz* format in the Supporting Information. All calculations were run in C_1 symmetry, even though all complexes have at least C_2 or C_s symmetry.

The Ru atoms in all complexes studied have a comparable environment in that they are surrounded by N atoms at distances between 2.08 and 2.11 Å, the sole outlier being the distance between Ru and the N-terminus of MeCN in $\mathbf{4}^{2+}$, which is 2.02 Å. It is also interesting to note that the pyridine group in $\mathbf{5}^{2+}$ lies parallel to the dppn long axis. This alignment replicates that seen in the crystal structure of the compound[18] and its corresponding dppz analogue.[15] The perpendicular conformation for $\mathbf{5}^{2+}$ does exist and is a stable (local) minimum; however, it lies 17.83 kJ/mol higher in energy. A similar number has been found in the past for the dppz analogues.[31] Therefore, assuming Boltzmann statistics, less than 0.1% will be in the perpendicular conformation.

In addition to the geometry minimizations, we also performed corresponding TD-DFT calculations for the singlet and the triplet ground states, both inside the polarizable continuum (PCM) approximation and from the corresponding optimized geometries.

The frontier orbitals for $\mathbf{5}^{2+}$ and further details are summarized in the Supporting Information. The calculated structure and UV—vis absorption spectrum for $\mathbf{5}^{2+}$ are given in Figure 6a. A comparison of this figure to the experimental spectrum in Figure 1 shows a semiquantitative agreement between experimentally observed and calculated transitions. The low-energy absorption manifold is due to a variety of ^{1}MLCT transitions from various Ru^{II} d orbitals to dppn. The transition at 359 nm is due to an MLCT to the pyridine ligand. We note that the lowest electronic transition would be from the HOMO located on the benzophenazine part of the dppn ligand to the LUMO localized across the entire dppn ligand; however, this transition does not appear in the UV—vis absorption spectrum due to the low oscillator strength (0.015; intensity 3480). The behavior of $\mathbf{4}^{2+}$ is very similar to that of $\mathbf{5}^{2+}$, and the corresponding data are summarized in the Supporting Information.

The electronic properties of $\mathbf{3}^{2+}$ are different from those of $\mathbf{4}^{2+}$ and $\mathbf{5}^{2+}$, due to a considerable contribution from bpy-based orbitals. The calculated structure and UV—vis absorption spectrum for $\mathbf{3}^{2+}$ are given in Figure 6b. A comparison of this figure to the experimental spectrum in Figure 1 again reveals a semiquantitative agreement between the experimentally observed and calculated transition energies. On the other hand, the intensities are not reproduced as well. This is not surprising given that these are a higher order property. As for the tpm-based complexes $\mathbf{4}^{2+}$ and $\mathbf{5}^{2+}$, theoretically the lowest electronic transition in $\mathbf{3}^{2+}$ is from the HOMO located on the benzophenazine part of the dppn ligand to the LUMO localized across the entire dppn ligand; however, this transition does not appear in the experimental UV—vis absorption spectrum due to the low oscillator strength (0.016; intensity 3500).

The calculated transitions for $\mathbf{3}^{2+}$ are given in Table 4. The corresponding orbitals for the six highest energy transitions are given in Figure 1S of the Supporting Information.

Comparing Figure 1S of the Supporting Information with the data in Table 4 and the experimental spectrum in Figure 1 shows that the theoretical assignment for the observed transitions is identical to the experimental one. The lowest energy absorption manifold is a combination of mixed ^{1}MLCT transitions from various Ru *d* orbitals to bipyridine and dppn ligands. The Ru—dppn transition is directed either to the entire dppn ligand (LUMO, LUMO + 4) or to the phenanthroline part of the dppn ligand (LUMO + 3, part of LUMO + 1). The absorption maximum at 345 nm is clearly a $^1\pi-\pi^*$ transition on the dppn moiety (vibrational progression is not included in the calculations). Calculated transitions for the other molecules studied confirm the similarities between the different Ru^{II}(dppn) complexes studied (see the Supporting Information).

To further elucidate the nanosecond absorption spectrum, we also performed TD-DFT calculations on the lowest triplet state for each of the complexes studied by first relaxing the geometry of the complexes on the triplet surface before performing the TD-DFT calculations. Here, we present the results for $\mathbf{3}^{2+}$ and $\mathbf{5}^{2+}$, but full results are given in the Supporting Information. By doing calculations on both the singlet and triplet states, we obtained the splitting between the ground state and the first excited triplet state, which is calculated to be 928.33 nm for $\mathbf{3}^{2+}$ and 932.43 nm for $\mathbf{5}^{2+}$. These numbers are consistent with TD-DFT calculations on these complexes performed from the

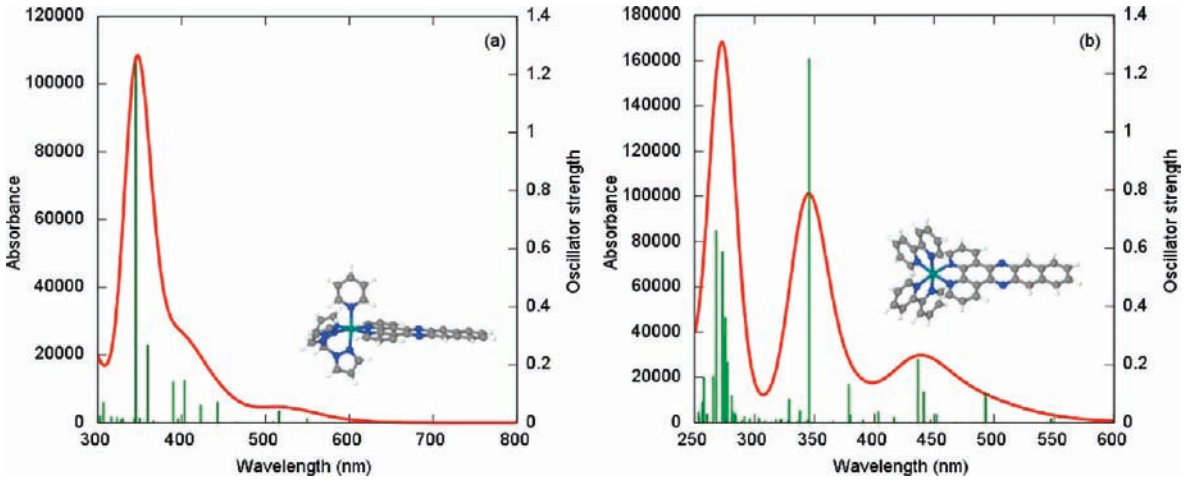

Figure 6. Calculated structures and absorption spectra, assuming an fwhm of Lorentzian bands of 3000 cm^{-1} for the singlet manifold of (a) $\mathbf{5}^{2+}$ and (b) $\mathbf{3}^{2+}$ in CH_3CN. See the text for details.

TABLE 4: Selected Calculated Electronic Transitions within the Singlet Manifold for the Spectrum of $\mathbf{3}^{2+}$ in MeCN[a]

no.	E (cm^{-1})	λ_{calcd}	oscillator strength	major contributions
5	20287.40	492.91	0.10	H − 2 → LUMO (89%) [Ru → dppn MLCT]
12	22667.56	441.15	0.10	H − 3 → L + 1 (10%), H − 3 → L + 3 (49%), H − 2 → L + 2 (29%) [mixed MLCT, Ru → bpy and Ru → phen part of dppn]
13	22913.56	436.42	0.22	H − 3 → L + 2 (41%), H − 2 → L + 1 (16%), H − 2 → L + 3 (30%) [mixed MLCT, Ru → bpy and Ru → phen part of dppn]
18	24793.65	403.32	0.04	H − 4 → LUMO (23%), HOMO → L + 4 (73%) [delocalized $\pi\pi^*$ dppn and $\pi\pi^*$ "benzphenazine"-to-"phen" fragments of dppn]
21	26412.42	378.60	0.13	H − 3 → L + 4 (61%), H − 2 → L + 3 (10%), H − 1 → L + 4 (12%) [MLCT Ru → dppn]
24	28945.01	345.48	1.25	H − 4 → LUMO (59%), HOMO → L + 4 (18%) [delocalized $\pi\pi^*$ dppn and $\pi\pi^*$ "benzphenazine"-to-"phen" parts of dppn]

[a] All transitions decomposed into the major orbital contributions relative to the HOMO (H) and the LUMO (L) of the system. The cutoff oscillator strength is 0.04. The HOMO is orbital number 175, and the LUMO is orbital number 176. Only transitions with more than 10% (or the largest) contribution are included.

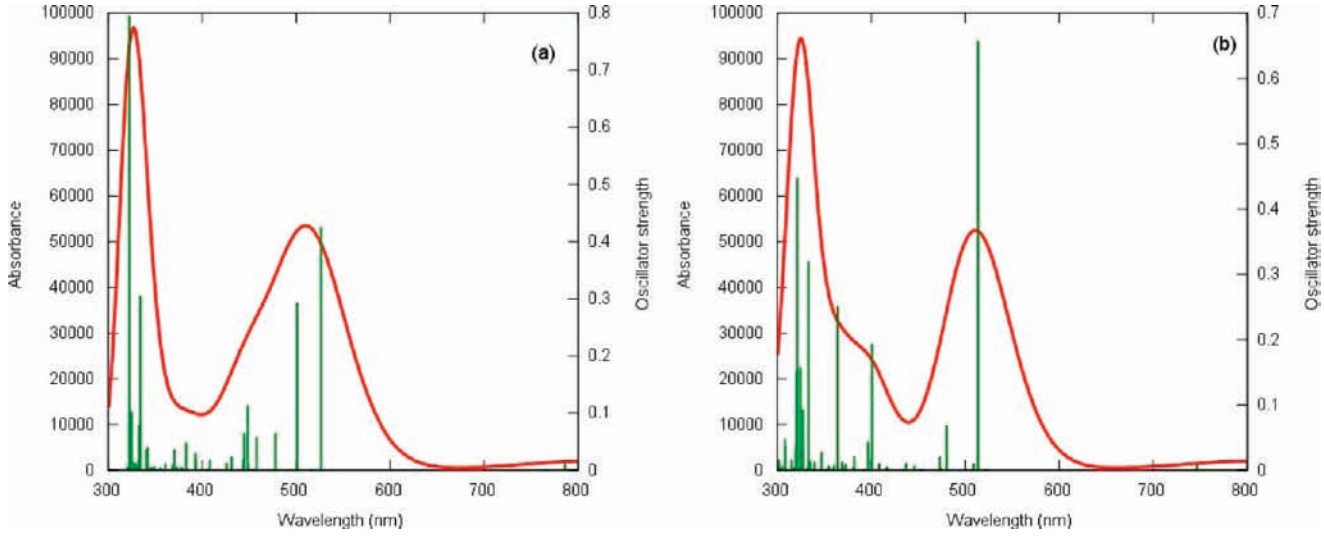

Figure 7. Calculated absorption spectrum for the lowest triplet state of (a) $\mathbf{3}^{2+}$ and (b) $\mathbf{5}^{2+}$. The fwhm of Lorentzian bands was set to 3000 cm^{-1}.

singlet state, where we only calculated triplet excited states. For all three complexes, this transition is dominated by the HOMO−LUMO transition. Thus, the lowest excitation in those complexes is $\pi-\pi^*$ in nature, and its calculated energy of 1.33 eV is in good agreement with the experimental value of 1.5 eV reported for the pydppn-based systems.[27]

The calculated electronic absorption spectra for the lowest triplet state of $\mathbf{3}^{2+}$ and $\mathbf{5}^{2+}$, $T_1 \rightarrow T_n$, are given in Figure 7 and are compared with the experimental spectra obtained in transient absorption experiments.

The spectrum of $\mathbf{5}^{2+}$ (Figure 7b) is most easily assigned in this case. There is a strong transition at 513 nm and a weaker transition at 480 nm, in agreement with the experimental spectrum given in Figure 2. A strong band at 332 nm is calculated, which is outside the detection limit for the flash photolysis experiment. We note that only 100 excited states

TABLE 5: Detailed Comparison of the Triplet Absorption Spectrum between Theory and Experiment for 5^{2+} [a]

experimental wavelength	theoretical wavelength	oscillator strength	major contributions
410	400.71	0.19	α, H − 4 → L (21%); β, H − 2 → L + 1 (31%), H → L + 3 (23%)
500 (shoulder)	480.14	0.07	H − 7 (β) → LUMO (β) (63%), H − 4 (β) → LUMO (β) (17%)
540	513.53	0.66	α, H → L + 3 (36%); β, H − 4 → L (24%) (ππ* dppn)

[a] All wavelengths are given in nanometers. All transitions decomposed into the major orbital contributions relative to the HOMO (H) and LUMO (L) of the system. Selected orbital schematics are given in Figure 8.

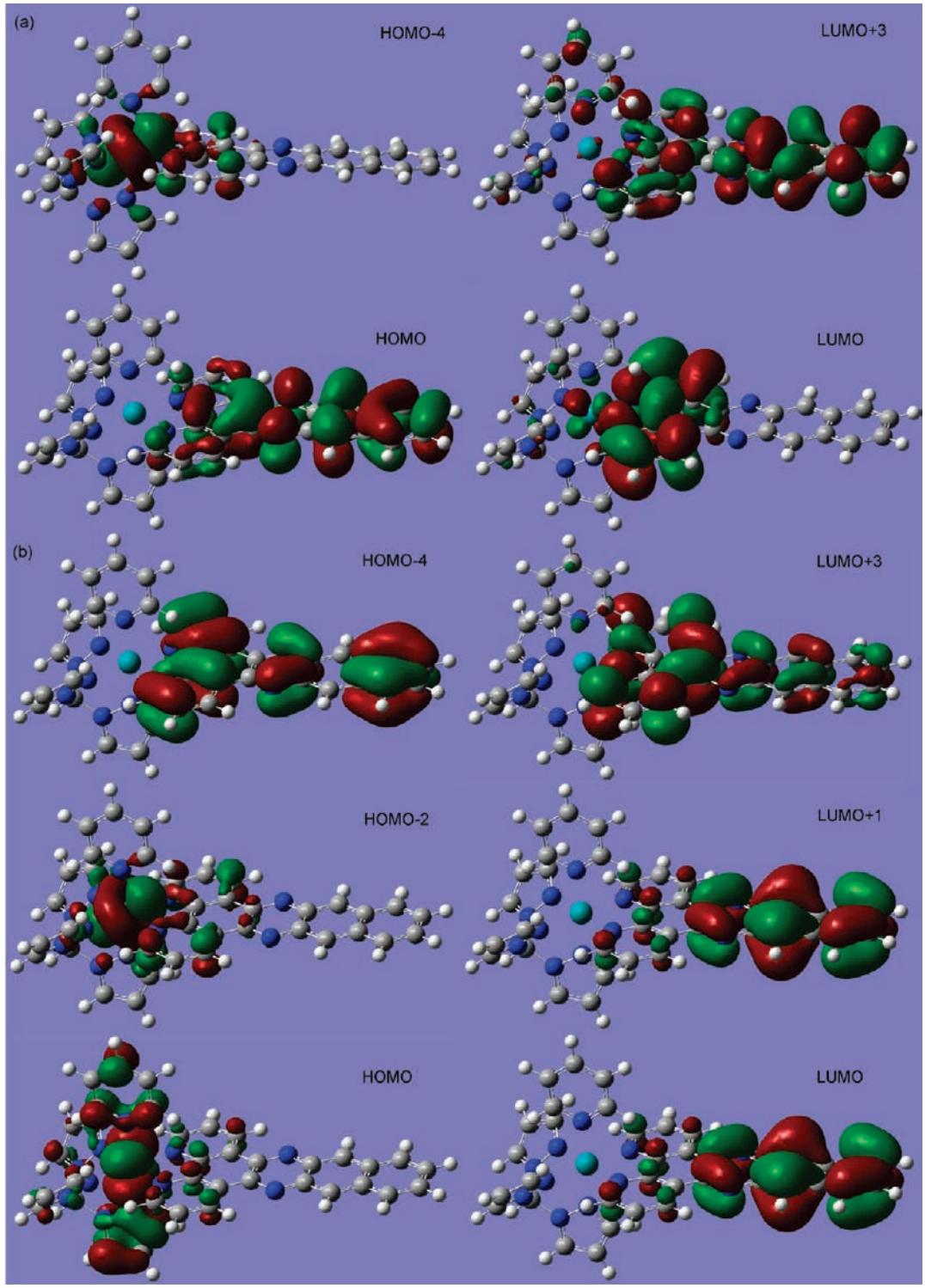

Figure 8. Selected orbitals of the triplet manifold of 5^{2+}: (a) orbitals on the α spin manifold, (b) orbitals on the β spin manifold.

were calculated, which means that no transitions below 300 nm are found. The orbital breakdown of these two transitions is given in Table 5. Cartoons of the orbitals involved are given in Figure 8. These schematics clearly show that the transition around 540 nm in the experimental spectrum is indeed a dppn-based $\pi-\pi^*$ transition, while the peak at 410

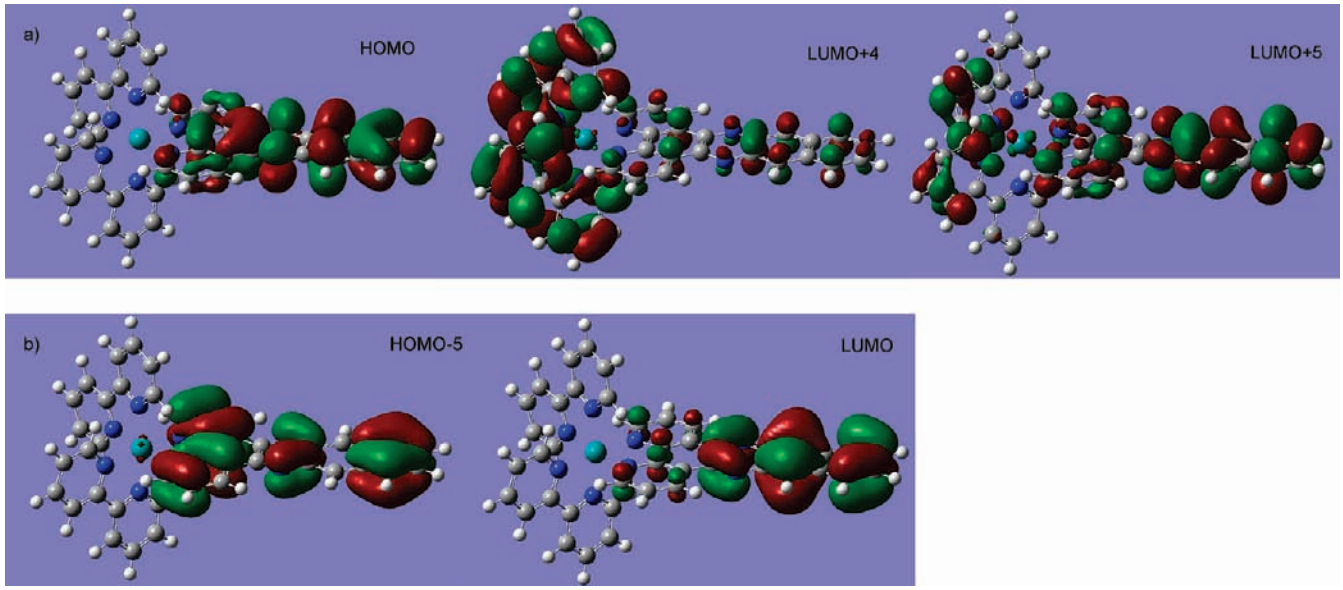

Figure 9. Orbitals involved in the lowest electronic transitions in the triplet state of $\mathbf{3}^{2+}$: (a) orbitals on the α spin manifold, (b) orbitals on the β spin manifold.

TABLE 6: Comparison of the Triplet Absorption Spectrum between Theory and Experiment for $\mathbf{3}^{2+}$ [a]

experimental wavelength	theoretical wavelength	oscillator strength	major contributions
530	526.38	0.42	α, H → L + 4 (64%); β, H − 5 → L (15%)
500	500	0.29	α, H → L + 5 (49%), H → L + 4 (20%); β, H − 5 → L (12%)
475	448.37	0.11	H − 2 (α) → L + 2 (α) (14%); H − 1 (β) → L + 1 (β) (53%)

[a] All wavelengths are given in nanometers. All transitions decomposed into the major orbital contributions relative to the HOMO (H) and LUMO (L) of the system. Selected orbital schematics are given in Figure 9.

nm appears to be predominantly an MLCT transition from the Ru metal center to the dppn ligand.

The calculated absorption spectrum of the lowest triplet state of $\mathbf{3}^{2+}$, showing a strong transition at 526 nm and weaker transitions at 500 and 448 nm, is in very good agreement with the experimental spectrum given in Figure 2. See Table 6 and Figure 9. The assignment for the spectrum of $\mathbf{3}^{2+}$ is complicated by the presence of three diimine ligands—two bipyridine ligands and one dppn. Since these ligands possess extensive π-systems, significant contributions from both bpy- and dppn-based manifolds could be anticipated. The reader is referred to the Supporting Information for more details.

It is clear from the calculations that the lowest triplet excited state in compounds $\mathbf{3}^{2+}$, $\mathbf{4}^{2+}$, and $\mathbf{5}^{2+}$ is a intra-dppn $\pi\pi^*$ transition. The possible mechanisms for the solvent-dependent effects seen in the excited-state lifetimes of the dppn-based complexes are currently being further investigated. It is tempting to conclude that—in much the same way as the emissive excited states of Ru^{II}(dppz) and Re^{I}(dppz) units are deactivated by close-lying alternative states—participation of one or more further excited states in the dppn-based complexes modulates the excited-state behavior of these systems. However, the DFT calculations presented herein indicate that while these complexes support many higher states that lie very close together in energy, these are energetically inaccessible from the lowest singlet and triplet manifolds at room temperature. This may be because the present calculations do not take into account specific effects such as hydrogen-bonding, which are known to be important in the photophysics of such complexes.[20] Experimental and computational studies designed to investigate this hypothesis will form the basis of future reports.

Conclusions

A detailed spectroscopic and computational study has been undertaken to characterize the photophysical properties of Ru^{II}(dppn)-based complexes. In contrast to Ru^{II}(dppz) systems, which display an MLCT-based lowest excited state, transient absorption studies revealed that the lowest excited state of *all* the Ru^{II}(dppn) complexes studied is a $^3\pi-\pi^*$ state, while DFT calculations confirm the nature of the excited state and the fact that it is centered on the dppn ligand.

Given that these compounds are photostable, have proven to be highly efficient photosensitizers of singlet oxygen with yields of >70%, and bind to DNA with high affinities, the possibility that complexes containing the Ru^{II}(dppn) moiety may find potential application as sensitizers for photodynamic therapy is currently being investigated. Furthermore, by using established methods,[15−18] $[Ru^{II}(tpm)(L)(dppn)]^{n+}$ complexes will be employed as building blocks in the creation of multifunctional oligonuclear complexes.

Experimental Section

Physical Measurements. UV−vis absorption spectra were measured on a Cary 50 Bio UV−vis spectrophotometer.

Nanosecond flash photolysis studies were conducted on the home-built setup. The tripled output of a Q-switched Nd:YAG laser, LS-2137U (LOTIS TII), was used as the excitation source (7 ns, 355 nm), while the probing was performed with a steady-state 150 W Hamamatsu Arc Xe lamp. The probe beam was detected by a monochromator equipped with a home-built detector unit, based on an FEU-118 PMT. The detector current output was coupled into a Tektronix TDS 3032B digital oscilloscope and subsequently transferred to the computer. The

instrumental response function is estimated as ca. 22 ns fwhm. Sample solutions in MeCN were degassed by the freeze−pump−thaw technique in 10 mm quartz cells and subsequently saturated with argon. Sample solutions in water were deoxygenated with the pump−thaw technique (without freezing the sample) in 10 mm quartz cells and subsequently filled with argon. Additionally, for a solution of 4 μM in MeCN, one data set was obtained in air-equilibrated conditions to illustrate oxygen quenching of the excited state. The excitation energies and sample concentrations used were 2.5−5 mJ and 20−35 μM, respectively, to obtain the shape of the transient spectra. To obtain reliable excited-state lifetimes, the excitation energies and sample concentrations were further reduced to 1.3−2.6 mJ and 4−7 μM, respectively, to avoid the self-quenching effect.

The analysis of time-resolved data to obtain decay lifetimes was performed using Igor Pro software (WaveMetrics, Inc.). The decay kinetics were fitted to the exponential decay law using the least-squares algorithm built into Igor Pro. Global fitting was applied to analyze simultaneously decay kinetics obtained for numerous spectral points, which considerably increased the reliability of the lifetime values obtained.

Singlet Oxygen Measurements. The luminescence of singlet oxygen ($^1\Delta_g$ O_2) was initiated by photoexcitation of metal complexes at room temperature in air-saturated CH_3CN solutions using the third harmonic of a Nd:YAG laser (355 nm, 7 ns). The luminescence was detected by a liquid nitrogen cooled germanium detector/amplifier (Applied Detector Corp., 403HS) close-coupled to the laser photolysis cell in right-angle geometry. A 1 mm thick, 20 mm diameter piece of AR-coated silicon (II−IV Inc.) was placed between the diode and cell to act as a cutoff filter for light below 1100 nm. The 403HS power supply bias voltage was operated at 450 V. The amplifier output was ac coupled to the digitizer. The output was displayed on a Tektronix TDS 380 digitizing oscilloscope. Data processing was performed on an IBM PC using in-house-developed software.

The quantum yield of $^1O_2$ production was determined by comparing the slopes of the linear plots of initial emission intensity vs laser energy for optically matched solutions (λ_{exc} = 355 nm) of the compounds under study and that of the standard (phenalenone, $\phi(^1O_2) = 95\%$).

DFT Calculations. The calculations were performed using the SMP version of the Gaussian 03 program package[32] with the B3LYP functional method.[33] Gaussian was compiled using the Portland Compiler, version 7.0-5, with the GOTO implementation (version 1.2.6) of BLAS[34] on the EMT64 architecture. In all calculations we used the Stuttgart/Dresden pseudopotential on Ru and the D95 V basis set on all other atoms.[35,36] The optimization included solvent effects treated via the polarizable continuum model[37] and the united atom topological model[38] applied to radii optimized at the Hartree−Fock 6-31(d) level of theory. This set of radii was used to retain compatibility with the implementation of PCM in earlier versions of Gaussian. We had significant difficulties converging the strucutures of the molecules, even though each electronic structure step converged quickly. It was realized that this was caused by numerical noise in the electronic energies. This introduced in its turn numerical noise in the gradients with respect to changes in the geometry. Therefore, we changed the standard PCM parameters with OFAC=0.92 and RMIN=0.15 to obtain a smoother cavity and better convergence behavior. In addition, all calculations were performed using ultrafine integrals. After obtaining a converged geometry, we ran TD-DFT calculations[39] to obtain the electronic excited states for both the singlet and the triplet manifolds. Hereby, 100 states were needed to obtain excitation wavelengths at the blue end of the experimental data. In the TD-DFT calculations, the influence of the solvent was treated exactly the same as during the geometry optimizations. The spectra were generated using GaussSum.[40]

Acknowledgment. We gratefully acknowledge the financial support of BBSRC (J.A.T. and S.P.F.), EPSRC (J.A.W. and M.A.H.A.), and the Marie Curie Incoming International Fellowship (I.V.S.) and FRRF, Daresbury Laboratory, STFC, U.K., for beam time. We are indebted to Dr. R. Edge and Dr. S. Navaratnam for their assistance with singlet oxygen measurements. All calculations were performed on the Theoretical Chemistry Group cluster "Jupiter" and the central "Iceberg" cluster at the University of Sheffield. We are grateful to the reviewers for their helpful comments.

Supporting Information Available: Additional information as described in the text. This material is available free of charge via the Internet at http://pubs.acs.org.

References and Notes

(1) Sigman, D. S.; Bruice, T. W.; Mazumder, A.; Sutton, C. L. *Acc. Chem. Res.* **1993**, *26*, 98. Nordén, B.; Lincoln, P.; Akerman, B.; Tuite, E. DNA Interactions with Substitution-Inert Transition Metal Ion Complexes. In *Metal Ions in Biological Systems*; Sigel, A., Sigel, H., Eds.; Marcel Dekker: New York, 1996; Vol. 33. Erkkila, K. E.; Odom, D. T.; Barton, J. K. *Chem. Rev.* **1999**, *99*, 2777–2795. Moucheron, C.; Kirsch-De Mesmaeker, A.; Kelly, J. M. *J. Photochem. Photobiol., B* **1997**, *40*, 91.

(2) Metcalfe, C.; Thomas, J. A. *Chem. Soc. Rev,* **2003**, *32*, 214. Hannon, M. J. *Chem. Soc. Rev.* **2007**, *36*, 280. Zeglis, B. M.; Pierre, V. C.; Barton, J. K. *Chem. Commun.* **2007**, 4565.

(3) Pyle, A. M.; Long, E. C.; Barton, J. K. *J. Am. Chem. Soc.* **1989**, *111*, 4520. Franklin, S.; Barton, J. K. *Biochemistry* **1998**, *37*, 16093. Metcalfe, C.; Adams, H.; Haq, I.; Thomas, J. A. *Chem. Commun.* **2003**, 1152. Nordell, P.; Westerlund, F.; Wilhelmsson, L. M.; Nordén, B.; Lincoln, P. *Angew. Chem., Int. Ed.* **2007**, *46*, 2203.

(4) Rajput, C.; Rutkaite, R.; Swanson, L.; Haq, I.; Thomas, J. A. *Chem.—Eur. J.* **2006**, *12*, 4611. Oleksy, A.; Blanco, A. G.; Boer, R.; Usón, I.; Aymami, J.; Rodger, A.; Hannon, M. J.; Coll, M. *Angew. Chem., Int. Ed.* **2006**, *45*, 1227. Reed, J. E.; Arnal, A. A.; Neidle, S.; Vilar, R. *J. Am. Chem. Soc.* **2006**, *128*, 5992. Morgan, J. L.; Spillane, C. B.; Smith, J. A.; Buck, D. P.; Collins, J. G.; Keene, F. R. *Dalton Trans.* **2007**, 4333. Kieltyka, R.; Fakhoury, J.; Moitessier, N.; Sleiman, H. F. *Chem.—Eur. J.* **2008**, *14*, 1145–1154.

(5) Önfelt, B.; Lincoln, P.; Nordén, B. *J. Am. Chem. Soc.* **1999**, *121*, 10846. Önfelt, B.; Lincoln, P.; Nordén, B. *J. Am. Chem. Soc.* **2001**, *123*, 3630.

(6) Friedman, A. E.; Chambron, J.-C.; Sauvage, J.-P.; Turro, N. J.; Barton, J. K. *J. Am. Chem. Soc.* **1990**, *112*, 4960. Hiort, C.; Lincoln, P.; Nordén, B. *J. Am. Chem. Soc.* **1993**, *115*, 3448.

(7) Jenkins, Y.; Friedman, A. E.; Turro, N. J.; Barton, J. K. *Biochemistry* **1992**, *31*, 10809.

(8) Holmlin, R. E.; Barton, J. K. *Inorg. Chem.* **1995**, *34*, 7. Holmlin, R. E.; Stemp, E. D. A.; Barton, J. K. *J. Am. Chem. Soc.* **1996**, *118*, 5236. Holmlin, R. E.; Barton, J. K. *Inorg. Chem.* **1999**, *38*, 174.

(9) Stoeffler, H. D.; Thornton, N. B.; Temkin, S. L.; Schanze, K. S. *J. Am. Chem. Soc.* **1995**, *117*, 7119.

(10) Yam, V. W.-W.; Lo, K. K.-W.; Cheung, K.-K.; Kong, R. Y.-C. *J. Chem. Soc., Chem. Commun.* **1995**, 1191.

(11) Dyer, J.; Blau, W. J.; Coates, C. G.; Creely, C. M.; Gavey, J. D.; George, M. W.; Grills, D. C.; Hudson, S.; Kelly, J. M.; Matousek, P.; McGarvey, J. J.; McMaster, J.; Parker, A. W.; Towrie, M.; Weinstein, J. A. *Photochem. Photobiol. Sci.* **2003**, *2*, 542.

(12) Kuimova, M. K.; Sun, X. Z.; Matousek, P.; Grills, D. C.; Parker, A. W.; Towrie, M.; George, M. W. *Photochem. Photobiol. Sci.* **2007**, *6*, 1158.

(13) Yam, V. W.-W.; Lo, K. K.-W.; Cheung, K.-K.; Kong, R. Y.-C. *J. Chem. Soc., Dalton Trans.* **1997**, 2067.

(14) Hartshorn, R. M.; Barton, J. K. *J. Am. Chem. Soc.* **1992**, *114*, 5919.

(15) Metcalfe, C.; Adams, H.; Haq, I.; Thomas, J. A. *Chem. Commun.* **2003**, 1152.

(16) Metcalfe, C.; Haq, I.; Thomas, J. A. *Inorg. Chem.* **2004**, *43*, 317.

(17) Foxon, S. P.; Phillips, T.; Gill, M. R.; Towrie, M.; Parker, A. W.; Webb, M.; Thomas, J. A. *Angew. Chem., Intl. Ed.* **2007**, *46*, 3686.

(18) Foxton, S. P.; Metcalfe, C.; Adams, H.; Webb, M.; Thomas, J. A. *Inorg. Chem.* **2007**, *46*, 409.

(19) Lincoln, P.; Broo, A.; Nordén, B. *J. Am. Chem. Soc.* **1996**, *118*, 2644.

(20) (a) Olson, E. J. C.; Hu, D.; Hörmann, A.; Jonkman, A. M.; Arkin, M. R.; Stemp, E. D. A.; Barton, J. K.; Barbara, P. F. *J. Am. Chem. Soc.* **1997**, *119*, 11458. (b) Önfelt, B.; Lincoln, P.; Nordén, B.; Baskin, J. S.; Zewail, A. H. *Proc. Natl. Acad. Sci. U.S.A.* **2000**, *97*, 5708–5713.

(21) Coates, C. G.; Olofsson, J.; Coletti, M.; McGarvey, J. J.; önfelt, B.; Lincoln, P.; Nordén, B.; Tuite, E.; Matousek, P.; Parker, A. W. *J. Phys. Chem. B* **2001**, *105*, 12653.

(22) Önfelt, B.; Olofsson, J.; Lincoln, P.; Nordén, B. *J. Phys. Chem. A* **2003**, *107*, 1000.

(23) Olofsson, J.; önfelt, B.; Nordén, B. *J. Phys. Chem. A* **2004**, *108*, 4391.

(24) Brennaman, M. K.; Alstrum-Acevedo, J. H.; Fleming, C. N.; Jang, P.; Meyer, T. J.; Papanikolas, J. M. *J. Am. Chem. Soc.* **2002**, *124*, 15094.

(25) Brennaman, M. K.; Meyer, T. J.; Papanikolas, J. M. *J. Phys. Chem. A* **2004**, *108*, 9938.

(26) (a) Pourtois, G.; Beljonne, D.; Moucheron, C.; Schumm, S.; Kirsch-De Mesmaeker, A.; Lazzaroni, R.; Brédas, J.-L. *J. Am. Chem. Soc.* **2004**, *126*, 683. (b) Batista, E. R.; Martin, R. L. *J. Phys. Chem. A* **2005**, *109*, 3128.

(27) Yiu, Y.; Hammitt, R.; Lutterman, D. A.; Joyce, L. E.; Thummel, R. P.; Turro, C. *Inorg. Chem.* **2009**, *48*, 375.

(28) Franco, C.; Olmstead, J., III. *Talanta* **1990**, *37*, 905.

(29) Sentage, C.; Chambron, J.-C.; Sauvage, J.-P.; Pailous, N. *J. Photochem. Photobiol., B* **1994**, *26*, 165.

(30) Schatzschneider, U.; Niesel, J.; Ott, I.; Gust, R.; Alborzinia, H.; Wölfl, S. *ChemMedChem* **2008**, *3*, 1104.

(31) Waywell, P.; Gonzalez, V.; Gill, M. R.; Adams, H.; Meijer, A. J. H. M.; Williamson, M. P.; Thomas; J. A. Submitted for publication to *Chem. Eur. J.*

(32) Frisch, M. J.; Trucks, G. W.; Schlegel, H. B.; Scuseria, G. E.; Robb, M. A.; Cheeseman, J. R.; Montgomery, J. A., Jr.; Vreven, T.; Kudin, K. N.; Burant, J. C.; Millam, J. M.; Iyengar, S. S.; Tomasi, J.; Barone, V.; Mennucci, B.; Cossi, M.; Scalmani, G.; Rega, N.; Petersson, G. A.; Nakatsuji, H.; Hada, M.; Ehara, M.; Toyota, K.; Fukuda, R.; Hasegawa, J.; Ishida, M.; Nakajima, T.; Honda, Y.; Kitao, O.; Nakai, H.; Klene, M.; Li, X.; Knox, J. E.; Hratchian, H. P.; Cross, J. B.; Bakken, V.; Adamo, C.; Jaramillo, J.; Gomperts, R.; Stratmann, R. E.; Yazyev, O.; Austin, A. J.; Cammi, R.; Pomelli, C.; Ochterski, J. W.; Ayala, P. Y.; Morokuma, K.; Voth, G. A.; Salvador, P.; Dannenberg, J. J.; Zakrzewski, V. G.; Dapprich, S.; Daniels, A. D.; Strain, M. C.; Farkas, O.; Malick, D. K.; Rabuck, A. D.; Raghavachari, K.; Foresman, J. B.; Ortiz, J. V.; Cui, Q.; Baboul, A. G.; Clifford, S.; Cioslowski, J.; Stefanov, B. B.; Liu, G.; Liashenko, A.; Piskorz, P.; Komaromi, I.; Martín, R. L.; Fox, D. J.; Keith, T.; Al-Laham, M. A.; Peng, C. Y.; Nanayakkara, A.; Challacombe, M.; Gill, P. M. W.; Jonson, B.; Chen, W.; Wong, M. W.; Gonzalez, C.; Pople, J. A. *Gaussian 03*, revision C.02; Gaussian, Inc.: Wallingford, CT, 2004.

(33) Becke, A. D. *J. Chem. Phys.* **1993**, *98*, 5648–5652.

(34) Goto, K.; van de Geijn, R. A. *ACM Trans. Math. Software* [Online] *34* (3), Article 12. http://www.tacc.utexas.edu/resources/software/software.php (last accessed May 18, 2009).

(35) (a) Nicklass, A.; Dolg, M.; Stoll, H.; Preuss, H. *J. Chem. Phys.* **1995**, *102*, 8942–8952. (b) Cao, X. Y.; Dolg, M. *J. Chem. Phys.* **2001**, *115*, 7348–7355, and references therein.

(36) Dunning, T. H., Jr.; Hay, P. J. In *Modern Theoretical Chemistry*; Schaefer, H. F., III, Ed.; Plenum: New York, 1976; Vol. 3, pp 1−28.

(37) (a) Menucci, B.; Tomassi, J. *J. Chem. Phys.* **1997**, *106*, 5151–5158. (b) Cossi, M.; Barone, V.; Menucci, B.; Tomassi, J. *Chem. Phys. Lett.* **1998**, *286*, 253–260, and references therein.

(38) Barone, V.; Cossi, M.; Tomassi, J. *J. Chem. Phys.* **1997**, *107*, 3210–3221.

(39) (a) Strattmann, R. E.; Scuseria, G. E.; Frisch, M. J. *J. Phys. Chem.* **1998**, *108*, 4439. (b) Bauernschmidt, R.; Ahlrichs, R. *Chem. Phys. Lett.* **1996**, *256*, 454. (c) Casida, M. E.; Jamorski, C.; Casida, K. C.; Salahub, D. R. *J. Chem. Phys.* **1998**, *108*, 4439.

(40) O'Boyle, N. M.; Tenderholt, A. L.; Langner, K. M. *J. Comput. Chem.* **2008**, *29*, 839.

JP906716G